Determining Optimal Resolution for Urban Terrain Inputs to Microclimate Modeling

Melissa R. Allen-Dumas[1], Levi T. Sweet[1], Christa M. Brelsford[1]

[1]Oak Ridge National Laboaratory, One Bethel Valley Road, Oak Ridge, TN 37831

Key Points:

- The resolution of the urban parameters in a numerical weather model make a difference to the output of the model.
- The differences are small but meaningful.
- Including urban development in weather modeling for the future will necessitate addition of the morphology of new neighborhoods to existing ones, and the capability for representing this growth at the resolution appropriate to the study is important.[1]

Corresponding author: Melissa R. Allen-Dumas, allenmr@ornl.gov

[1] This manuscript has been authored by UT-Battelle LLC under contract DE-AC05-00OR22725 with the US Department of Energy (DOE). The US government retains and the publisher, by accepting the article for publication, acknowledges that the US government retains a nonexclusive, paid-up, irrevocable worldwide license to publish or reproduce the published form of this manuscript, or allow others to do so, for US government purposes.DOE will provide public access to these results of federally sponsored research in accordance with the DOE Public Access Plan (http://energy.gov/downloads/doe-public-access-plan).

Abstract

As the numerical weather prediction community seeks deeper understanding of multi-scale interactions among the atmosphere, human systems and the overall earth system, more explicit representation of surface terrain in these models has become necessary. While a great body of work has examined the differences in error and uncertainty of simulations at various horizontal grid resolution, no studies have been performed that compare the results of running the models at the same horizontal grid resolution but with different resolutions of surface terrain. We examine the differences in meteorological output from the Weather Research and Forecasting (WRF) model run at 270m horizontal resolution using 10m resolution urban terrain (morphology) inputs and 100m resolution inputs. We find that differences in urban terrain resolution may amplify or dampen the representation of shortwave absorption by low albedo concrete and asphalt and the re-radiation of this energy as heat to the neighborhood.

Plain Language Summary

As cities continue to grow, scientists search for ways to describe accurately both the effect that urban growth has on climate and how cities might be vulnerable to climate change. In order to understand these interactions, scientists can use weather models to represent how certain characteristics of urban areas, such as building height, neighborhood density, and green space, might affect local weather. In this study, we use those urban characteristics at two different resolutions as urban terrain inputs to the Weather Research and Forecasting model for a Washington D.C. neighborhood. Higher resolution representations of the neighborhood provide a more precise characterization of the urban surface, but take more time and data to be processed than those at lower resolutions. We compare the results of the weather model when it is given a higher resolution (10 meter) and a lower resolution (100 meter) representation of the urban terrain of the Washington, D.C. Waterfront neighborhood. We find small but meaningful differences between the two model simulations, and our results show that researchers must make decisions about whether these differences are negligible for their studies or if they require the use of more detailed representation of urban characteristics.

1 Introduction

While it has long been known that the variety of surface roughness elements in a set of weather model parameters imparts mathematically the most critical effects on the generation of a system's vertical wind profile and mixing layer depth (Oke, 1988), only recently has the introduction of more granular distinctions in land use and land cover within physical models opened new research for including the communication of a neighborhood's urban morphology to the natural environment within which it exists (Ching et al., 2009; Oleson et al., 2010). Urban and non-urban areas have different sensitivities to weather and climate suggesting that the best estimate of a climate change signal within an urban area must be obtained through explicitly representing the urban areas within weather and climate simulations (Best, 2006). Certainly, as the need for greater spatial detail and fidelity of atmospheric flow fields in numerical weather prediction models increases, these models must account for the influence of buildings, trees, and other morphological features within the urban boundary layer. For example, the vertical walls of buildings affect overall thermal properties of an urban area because they reflect and absorb shortwave radiation. Additionally, losses of infrared energy at night over built areas are diminished due to the decreased sky view factor below the roof level of the buildings (Shahmohamadi et al., 2011). Representing these morphological characteristics of urban areas as inputs to weather models provides a way for weather models to incorporate the influence on the local atmosphere of the complexities of spatial distributions of buildings of different shapes and sizes so that, for example, the impact of significant weather events such as heat waves can be estimated at neighborhood resolution (Ching et al., 2009).

As urban areas grow, geography, topography, climate, history, technology, policy, infrastructure, culture, and population demographics all influence growth and changes in urban morphology (Oliveira, 2016). This growth can take forms such as edge expansion, which occurs when a new urban patch appears on the contour of an existing neighborhood or infilling, which occurs when gaps inside a neighborhood become partially or totally filled with new growth (Sapena & Ruiz, 2015). These growth patterns, then, aggregate in different ways to the overall densification or sprawl of a city and can affect the local meteorology and the larger scale climate through changes in atmospheric patterns (Allen-Dumas et al., 2020).

A variety of urban environment modeling studies have been conducted using urban morphological representations at different scales. For example, Oleson et al. developed an urban parameterization for the representation of urban expansion and its interaction with the Earth system within the Community Land Model component of the Community Climate System Model (Oleson et al., 2010). The urban parameters are rendered in the model at 0.5°x 0.5°horizontal resolution and include height to width ratio, roof fraction, average building height, and pervious fraction of the urban canyon for each four urban density classes (tall building, high, medium and low density districts). This configuration of the Community Land Model has been used by numerous researchers for many scientific investigations. In particular, (Li et al., 2016) ran simulations with the model for the Continental United States to understand the impact of urban land use on climate at that scale.

Ching et al. (Ching et al., 2009) developed a suite of urban parameter inputs called the National Urban Database and Access Portal Tool (NUDAPT) at 1km horizontal resolution for the higher resolution capability of the Weather Research and Forecasting (WRF) model. The 132 parameters included account for physical quantities related to buildings such as plan area, plan area density, frontal area index and height to width ratio for every 5m vertical layer in the model. Among the vast research conducted with the WRF model using these parameters, Vahmani et al. (Vahmani et al., 2019) ran several urban heat mitigation scenarios in this configuration at 1.5km resolution that evaluated exposure to future heat extremes under differing future climate and population scenarios. With buildings and additional landscape characteristics at one centimeter resolution, Reza (Reza, 2019) used the ENVI-met model to simulate microclimate changes due to changes in urban structure, and evaluated the impact of a 1°C increase in ambient temperature on the energy use in the buildings in the neighborhood. Each of these studies produced insight into different scientific questions, and each used the models and the associated urban morphological representations available to them.

However, none of these experiments evaluated the difference that the resolution of the input morphology would make in the output that was achieved. This observation is notable because there are numerous studies exploring the benefits and consequences of various horizontal grid resolutions in micrometerological simulations, and it is reasonable to hypothesize that urban morphology resolution is equally important. For example, it may be critical to know how much difference the resolution of the urban terrain input makes for determining neighborhoods and households most at risk to heat extremes (Ishigami et al., 2008)under a given micrometerological simulation. Likewise, as cities grow through expansion, infill and building higher, the resolution at which this change can be represented to a weather model may be the key to understanding the impact of this growth on the local and the broader environment.

In this paper we show, as an example, the differences in WRF simulation output at 270m horizontal grid resolution between running the model with 10m neighborhood morphological inputs and running it with 100m morphological inputs. This work contributes to the important and growing literature on urban micrometerological modeling by elucidating the trade-offs between modeling expenses such as compute time and data requirements and the fidelity and resolution of the resulting simulations. We find small but meaningful differences between the simulations. Most notably, we see contrasts in the spatial distribution of temperature, humidity and wind between the two simulations, which may be important to estimating the full contribution of urban parameters to the thermal characteristics of a neighborhood in a city (Lee, 1984).

2 Materials and Methods

Two 1-month, three-domain, nested meteorological simulations were run for the month of July, 2010 using North American Regional Reanalysis (NARR) data (Mesinger et al., 2006) as initial and boundary conditions over urban terrain inputs at each of 10m and 100m resolution for the Washington, DC Waterfront neighborhood. The simulations used the Weather Research and Forecasting (WRF) model run on the Oak Ridge National Laboratory (ORNL) Summit and Cades supercomputers, respectively. The horizontal resolution for each of the model domains (from outermost to innermost) was 6750m (d01), 1350m (d02) and 270m (d03), respectively; and each contained 29 vertical levels with the model top at 100 hPa as defined by the NARR input. The number of grid cells in each domain is given in Table 1.

The urban terrain inputs at 10m and 100m resolution were generated using shapefiles of building footprints and corresponding building heights acquired from Open Data DC (OpenDataDC, 2021) for the year 2015. From these shapefiles, urban parameters were calculated following the methodology of the NUDAPT project (Ching et al., 2009). For this calculation, a tool was produced using the Python coding language, which output files for the urban topography at both 10m and 100m resolution as WRF-readable binary files integrable with WRF using the established NUDAPT paths in the WRF simulation environment.

Landcover characteristics used were those obtained from the US Geological Survey National Land Cover Database (NLCD) (Homer et al., 2012) at 30 m resolution and included in the WRF pre-processing geography input package. The NLCD provides urban land classifications such as percentage impervious surface, percentage of tree canopy cover and percentage of coverage of constructed materials.

The timestep used for the outermost (6750 m) domain was 10 seconds. The timestep for each nested grid was in the same ratio to the outer domain as was its spatial dimension. Nesting ratios for the simulations were 5:1. This ratio is based on recommendations from Werner (Werner, 2017) to align U and V velocities calculated at the edges of the parent-to-child Arakawa C-grids with mass quantities calculated at the centers of these cells. The simulations were run from June 30 through July 21, 2010, and each included a 24-hour model spinup before the 10-day period evaluated here.

Physics packages for WRF were chosen based on optimum packages for urban scenarios. The most significant packages are shown in Table 2. WRF output was postprocessed so that its Coordinated Universal (UTC) timestamps aligned with local Eastern Daylight time for comparison with observations at local time from the archives accessed for both the Weather Underground data reported for the Reagan National Airport (DCA) (Weather Underground, 2010) and the National Centers for Environmental Information archives (Menne et al., 2012) for the National Arboretum. Additionally, 10m windspeed and direction were derived from U and V, and relative humidity was calculated using 2m temperature, surface pressure and 2m water vapor mixing ratio inputs to the NCAR Command Language (NCL) relhum function based on (Murray, 1966) and the SH2RH function provided by the R "humidity" package (Cai, 2019).

Table 1. Numbers of grid cells for simulations' nested domains. Two simulations were run. The first used urban terrain at 10m resolution in the d03 domain; the second used urban terrain at 100m in the d03 domain.

d01	d02	d03	d03
99x93	145x135	100x120	100x120

Table 2. Physics packages for WRF simulation

Domain	Microphysics	Radiation	Cloud Fraction	Cumulus	Surface Physics	Land	PBL	Urban Params
d01	Single Moment 3-class	New Goddard	Xu-Randall	Kain-Fritsch	Monin-Obukhov	Noah	BouLac	Urban Canopy
d02	Single Moment 3-class	New Goddard	Xu-Randall	Kain-Fritsch	Monin-Obukhov	Noah	BouLac	Urban Canopy
d03	Single Moment 3-class	New Goddard	Xu-Randall	Betts-Miller-Janjic	Monin-Obukhov	Noah	BouLac	10m morphs
d03	Single Moment 3-class	New Goddard	Xu-Randall	Betts-Miller-Janjic	Monin-Obukhov	Noah	BouLac	100m morphs

It is known that numerical weather prediction models contain inherent biases. When these models are used for official forecasts, the biases must be removed before the forecasts can be distributed (Davis, 2004). For experimentation to evaluate differences in output due to changes in parameters, as we have done here, it is enough to know how the model output compares to measurements so that the output is referenced with regard to an actual weather event. To acknowledge the bias of the simulated data we present with respect to measurements, spatial averages of temperature, humidity and wind for July 1-10, 2010 over the 2015 Waterfront neighborhood were compared to those measured at the Reagan National Airport (DCA), which is located across the Potomac and southwest of the neighborhood. Additionally, the temperature spatial averages were compared to those recorded at the National Arboretum located to the northeast of the neighborhood. Figures 1, 2 and 3 show that daily maximum, minimum and average temperatures track below the DCA measurements by about 10°F or more and lead the observations by about a day in trend. Maximum and average temperatures track more closely with the National Arboretum values, while minimum temperature values are farther below those measured at the National Arboretum. Simulated relative humidity is overestimated in each case as compared to the DCA measurements and by as much as 40% for the minimum. Some of the bias, such as systematic cold bias and overestimation of humidity during the summer and high bias of wind speed (Figure 5) over all seasons, is generally characteristic of the WRF model (García-Díez et al., 2013; Pan et al., 2018; Bughici et al., 2019). Some of the additional bias may be due to the sensitivity of the model to the difference in the urban terrain between that which would have been present in 2010 and that which was used (2015) in the model simulation (Wang et al., 2011). Nevertheless, the difference in the spatially averaged model results from the simulations run with the two resolutions of the urban terrain showed much less difference from each other and demonstrated that the simulation results were likely not significantly affected by initial conditions.

Spatially averaged planetary boundary layer height ranged from a lowest minimum of 50m to a highest maximum of 1750m throughout the 10-day study period, a range similar to that shown in the average July, 2011 (a month with related record temperatures to those of July, 2010) observations over the Baltimore-Washington area during the D.C. DISCOVER-AQ campaign (Hegarty et al., 2018). Differences in the maxima and minima of the simulations with each resolution morphology were nearly 375 meters at the maximum on July 8 (10m terrain showing the highest level) and 50 meters for the minimum on July 7 (100m terrain with higher boundary layer), respectively. The largest difference in maximum temperature between the two simulations occurs on July 8 (10m simulation warmer) as well, which corresponds to the large difference in the boundary layer on that day. Other small differences between the boundary layer simulation outputs are shown throughout the 10-day period, but are less drastic.

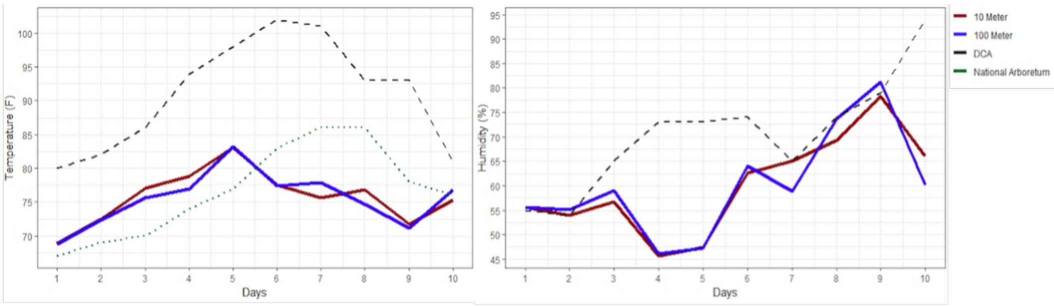

Figure 1. Maximum temperature and humidity, spatial averages over 10m (red line) and 100m (blue line) morphologies for Washington, DC Waterfront neighborhood run with July 1-10, 2010 meteorological initial and boundary conditions. Observations from the Reagan National Airport (DCA) are shown in black (dashed line) and observations from the National Arboretum are shown in green (dotted line) for comparison.

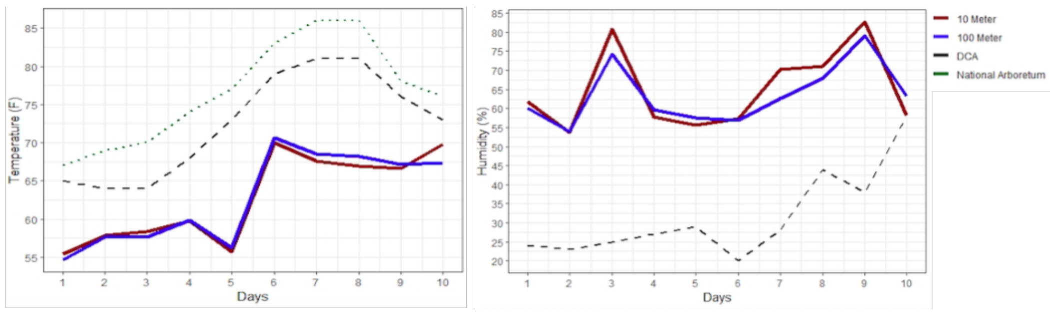

Figure 2. Minimum temperature and humidity, spatial averages over 10m (red line) and 100m (blue line) morphologies for Washington, DC Waterfront neighborhood run with July 1-10, 2010 meteorological initial and boundary conditions. Observations from the Reagan National Airport (DCA) are shown in black (dashed line) and observations from the National Arboretum are shown in green (dotted line) for comparison.

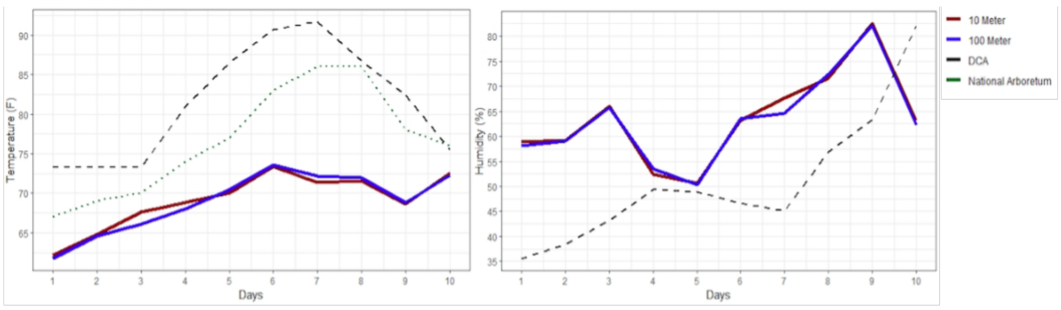

Figure 3. Average temperature and humidity, spatial averages over 10m (red line) and 100m (blue line) morphologies for Washington, DC Waterfront neighborhood run with July 1-10, 2010 meteorological initial and boundary conditions. Observations from the Reagan National Airport (DCA) are shown in black (dashed line). Observations from the National Arboretum in this case are for observations that occurred sometime during each day between the minimum and maximum temperatures, but are not necessarily averages. These values are shown in green (dotted line).

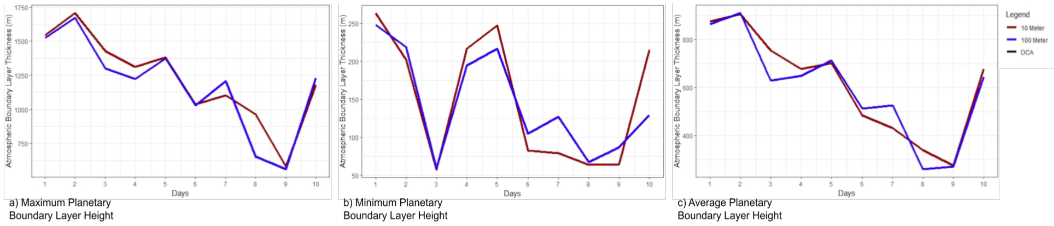

Figure 4. Spatially averaged planetary boundary layer (PBL) heights over 10m and 100m morphologies for Washington, DC Waterfront neighborhoods run with July 1-10, 2010 meteorological initial and boundary conditions

Wind pattern comparisons (Figure 5) show that for simulations run with both 10m and 100m urban terrain, the wind direction is fairly consistent from the west southwest direction. Variation in wind speed counts occur mostly in the middle of the range of the wind speed data. DCA measured data shows more variability in wind direction with most of the wind coming from directly south and directly north. Wind speeds from DCA are also much slower compared to those simulated over each urban terrain input. Differences between the simulated and the observed wind speed and direction may be due in part to the distance between DCA and the Waterfront neighborhood, and to the difference in respective fetch (Fagherazzi & Wiberg, 2009).

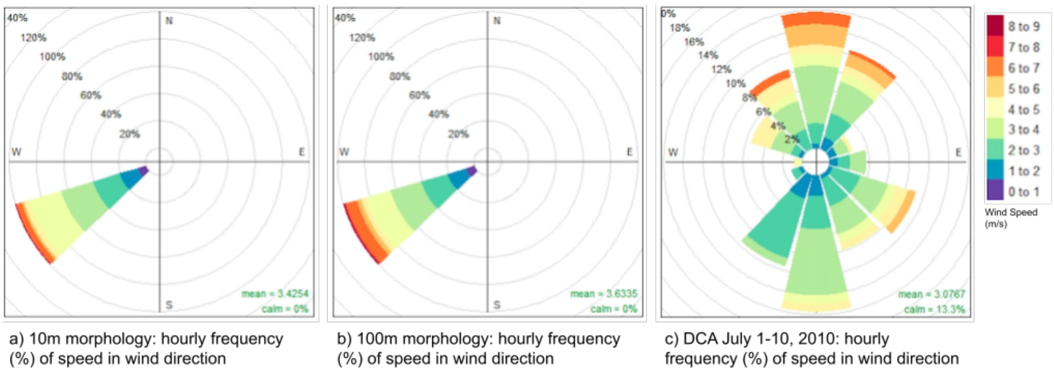

Figure 5. Hourly wind over 10m and 100m morphologies for Washington, DC Waterfront neighborhood run with July 1-10, 2010 meteorological initial and boundary conditions

3 Results and Discussion

Records beginning in the late 1800s for Washington, DC show that its population has grown continuously, and its land surface radius has expanded with greater heat-absorbing paved and built area leading to increasing heat records within the city and intensifying its urban heat island effect (Samenow, 2012). During the summer of 2010, Washington, DC recorded temperatures that surpassed 98°F (37°C) on 11 days, reaching a peak of 102°F (39°C) on July 6 and 7. July 6 of that year broke two records: the earliest 100°reading in a day, occurring before noon, and the longest uninterrupted stretch of temperatures above 100°F (7 hours).

Figure 6 shows the spatial distribution over the Washington, DC Waterfront neighborhood of the averaged daily maximum temperature over the ten days of the 2010 heatwave using urban terrain inputs at each of 10m and 100m. While the temperature distribution over the neighborhood looks similar for the a) 10m and the b) 100m renderings, the difference plot shows locations up to 0.59°F cooler in the 100m result as compared to the 10m result. In the simulation result using the 10m terrain, the largest area over the built section shows the highest temperatures. In the result simulated with the 100m terrain, none of the area reaches the highest temperature. A possible explanation for this difference is that the higher resolution building inputs allowed the darkly-colored and highly heat absorbent impervious surfaces to be exposed to the model, feeding the radiation from these surfaces back into the overall system (Lee, 1984).

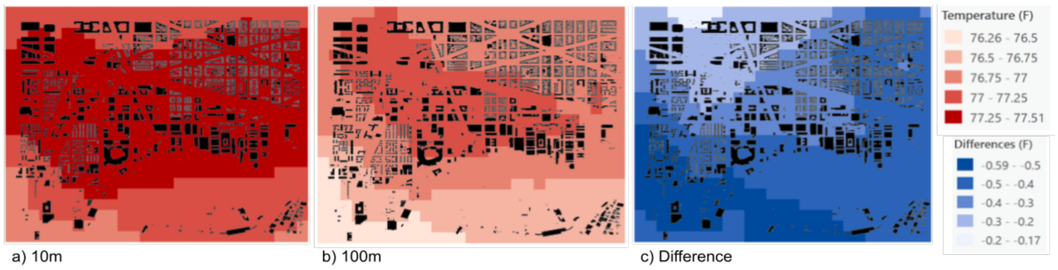

Figure 6. Time-averaged maximum temperature over a) 10m and b) 100m morphologies for the Washington, DC Waterfront neighborhood run with July 1-10, 2010 meteorological initial and boundary conditions. The c) difference panel is the result of subtracting the values produced by the simulation run with the 10m morphology from the values produced by the simulation run with the 100m morphology.

However, the urban heat island effect has its greatest impact on night time temperatures, as heat is essentially trapped in the urban core during the day rather than escaping into space (Samenow, 2012). The 2010 and 2011 heatwaves in Washington, DC were recorded as having both the most and the second most nights above 80°(7 in 2011 and 4 in 2010). Figure 7 shows the time-averaged minimum temperature over the Waterfront neighborhood for the 10 day heatwave. The largest differences between the results appears in the northern portion (up to 0.16°warmer for the 100m simulation) of the neighborhood, and in the southern portion (as much as .018°cooler in the 100m simulation). The highest minimum temperatures for both simulations are over the waterways in the southwest corner of the neighborhood, a result that agrees with (Mikolaskova, 2009) and (Scheitlin, 2013), who demonstrated that land locations experience higher maximum temperatures and lower minimum temperatures than locations over water.

Average daily temperatures averaged over the 10 day heat wave show variation as well across the Waterfront neighborhood (Figure 8). The most obvious difference between the results of using the two different morphology resolutions is the extent of the salmon colored region shown in panel a) (10m resolution morphology), which covers most of the built area of the neighborhood. In the result that used the 100m morphology, this temperature range covers only an area centered on the Nationals stadium (circular building near the Anacostia River), potentially indicating that, as with the maximum temperature result, the higher resolution morphology exposed more heat-absorbent land area that, on average, maintains a higher temperature than the remaining northeast part of the neighborhood. Nevertheless, the differences observed in the spatial distribution of maximum, minimum and average temperature over the Waterfront neighborhood represented at the two different resolutions are at most 0.25°to 0.6°F. Thus, temperature dependent planning choices that can be made within this margin of error may best be modeled using the more quickly generated urban terrain inputs at the coarser resolution.

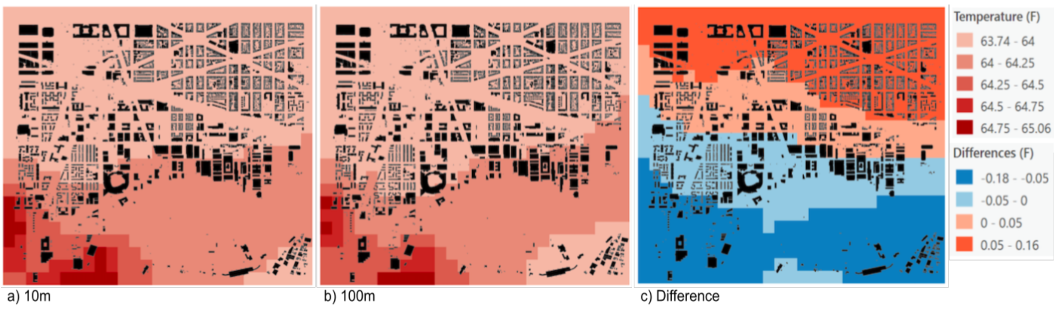

Figure 7. Time-averaged minimum temperature over a) 10m and b) 100m morphologies for the Washington, DC Waterfront neighborhood run with July 1-10, 2010 meteorological initial and boundary conditions. The c) difference panel is the result of subtracting the values produced by the simulation run with the 10m morphology from the values produced by the simulation run with the 100m morphology.

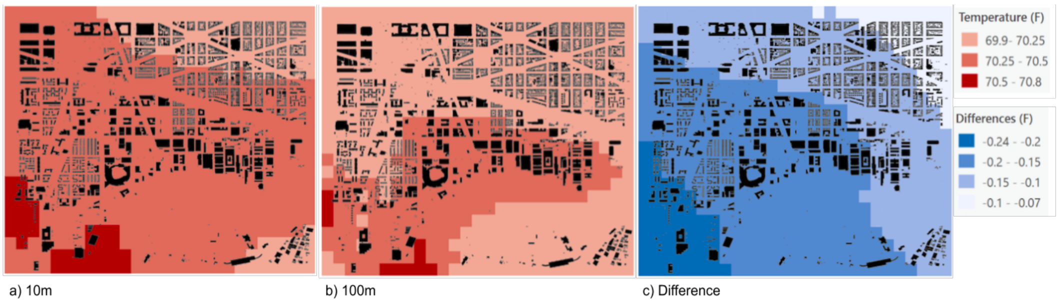

Figure 8. Time-averaged average temperature over a) 10m and b) 100m morphologies for the Washington, DC Waterfront neighborhood run with July 1-10, 2010 meteorological initial and boundary conditions. The c) difference panel is the result of subtracting the values produced by the simulation run with the 10m morphology from the values produced by the simulation run with the 100m morphology.

Spatial variability for relative humidity (Figure 9) across the Waterfront neighborhood ranged from 57.09% to 59.68% in both the 10m and the 100m resolution terrain simulations. The largest difference between the simulations was 0.53%, with the 100m simulation showing the higher humidity on the western side of the neighborhood along the Washington Channel. The simulated northwest area of the neighborhood at 100m was drier by 0.21% than that of the simulated area with 10m resolution terrain.

Wind direction over both the 10m and the 100m resolution urban terrain is generally from the west southwest as was seen in the wind rose comparison (Figure 5) in section 2. However, slight differences in the time averaged maximum wind speeds and direction over the two different terrain resolutions shown in Figure 10 indicate a shift from mostly west to more northwest originating wind, especially as the air exits the urban area and flows over the Anacostia River. Wind speed in both simulations is slower over the built area and faster over the water, a result that concurs with the tendency of warm air to stagnate in urban canyons and speed up over areas that are less built up (Shahmohamadi et al., 2011). The largest differences in wind speed between the two simulations occur over the northwestern portion of the Waterfront neighborhood, at which the 100m resolution terrain simulation produces the slower of the two maximum speeds in that area.

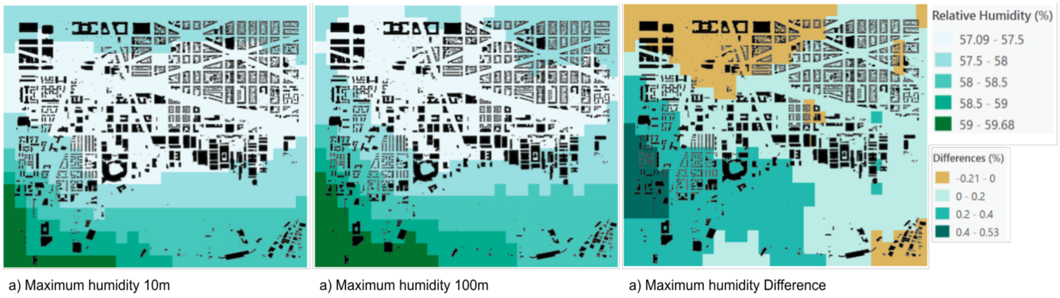

Figure 9. Time averaged maximum relative humidity over a) 10m and b) 100m morphologies for the Washington, DC Waterfront neighborhoods run with July 1-10, 2010 meteorological initial and boundary conditions. The c) difference panel is the result of subtracting the values produced by the simulation run with the 10m morphology from the values produced by the simulation run with the 100m morphology.

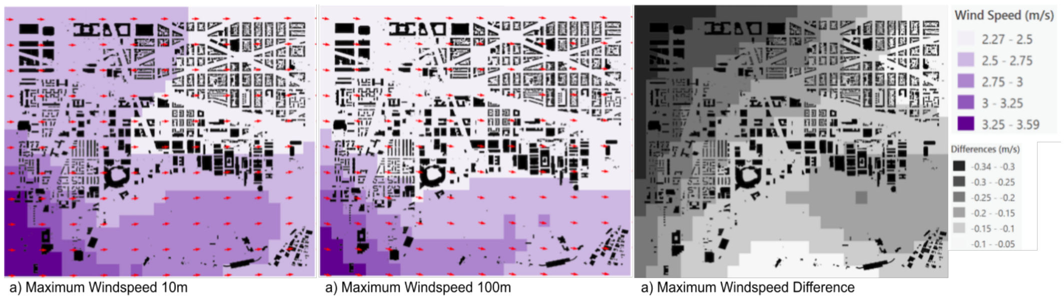

Figure 10. Time averaged maximum windspeed and direction over 10m and 100m morphologies for Washington, DC Waterfront neighborhoods run with July 1-10, 2010 meteorological initial and boundary conditions

4 Conclusions and Future Work

We have shown that for simulations at 270m horizontal grid resolution over a neighborhood in Washington, DC, the spatial variability in temperature, humidity and wind speed and direction across the neighborhood changes with the resolution of the urban morphology used, and that the simulated results show different areas of the neighborhood up to 0.6°F warmer or cooler, 0.5% wetter or drier, and 0.3m/s windier or calmer depending on the resolution of the morphology used in the simulation. These differences may be negligible for the pursuit of some types of knowledge, but may be very meaningful for others. One possible explanation for the spatial patterns we saw with this experiment was that dark impervious surfaces such as asphalt were revealed between the buildings at 10m resolution whereas those areas may have been represented to the model as built (and lighter colored) areas at 100m resolution. Thus, for including new morphology scenarios in such models that build on modeling growth in impervious surfaces in response to population shift scenarios (Brelsford et al., 2020), or the impact of building regulations and codes on the dimensions of buildings, their geometrical form and arrangement and their energy efficiency (Asimakopoulos, 2001), possibly higher morphological resolution is necessary. Contrastingly, for understanding the ways in which a neighborhood's demography may affect the type of buildings that make up a new neighborhood and their packing density within it (Oke, 1988), 100m may be sufficient.

Researchers and urban planners have begun to develop future scenarios, pathways and plans, and to implement projects that improve urban sustainability and urban resilience (McPhearson et al., 2016). Understanding the resolution at which urban terrain inputs to weather models makes a difference in those scenarios and pathways will help planners choose modeling approaches that provide the most useful and time-efficient information for the solutions that are needed.

In conclusion, we show that horizontal resolution differences in terrain inputs to numerical weather models do result in differences, especially in the spatial variability of micrometeorological parameters. However, the study did not investigate the appropriateness of the numerical techniques applied the (sub-kilometer) horizontal grid resolution at which the simulations were performed, and thus, the results still carry some uncertainty (Wedi, 2014). Nevertheless, the results presented here pose interesting new questions about the required resolution of the model's surface terrain, especially with regard to urban interactions with the local to regional atmosphere.

Acknowledgments

This research was sponsored by the DOE Office of Science as a part of the research in Multi-Sector Dynamics within the Earth and Environmental System Modeling Program. It used resources of the Oak Ridge Leadership Computing Facility at the Oak Ridge National Laboratory, which is supported by the DOE Office of Science. The authors especially appreciate the encouragement of Integrated Multiscale Multisector Modeling (IM3) Principal Investigator, Jennie Rice, of Pacific Northwest National Laboratory, to perform the experiments reported here. WRF-generated data from each of the simulations will be available through data DOI at Zenodo.

References

Allen-Dumas, M. R., Rose, A. N., New, J. R., Omitaomu, O. A., Yuan, J., Branstetter, M. L., ... others (2020). Impacts of the morphology of new neighborhoods on microclimate and building energy. *Renewable and Sustainable Energy Reviews*, *133*, 110030.

Asimakopoulos, D. N. (2001). *Energy and climate in the urban built environment.* Earthscan.

Best, M. (2006). Progress towards better weather forecasts for city dwellers: from short range to climate change. *Theoretical and Applied Climatology*, *84*(1), 47–55.

Brelsford, C., Coon, E. T., Moran, E., & Allen-Dumas, M. (2020). Urban scaling as validation for predictions of imperviousness from population. *Geophysical Research Letters*, *47*(23), e2020GL089742.

Bughici, T., Lazarovitch, N., Fredj, E., & Tas, E. (2019). Evaluation and bias correction in wrf model forecasting of precipitation and potential evapotranspiration. *Journal of Hydrometeorology*, *20*(5), 965–983.

Cai, J. (2019). *Humidity.* `https://cran.r-project.org/web/packages/humidity/humidity.pdf`.

Ching, J., Brown, M., Burian, S., Chen, F., Cionco, R., Hanna, A., ... others (2009). National urban database and access portal tool. *Bulletin of the American Meteorological Society*, *90*(8), 1157–1168.

Davis, J. T. (2004). Bias removal and model consensus forecasts of maximum and minimum temperatures using the graphical forecast editor. *NOOA NWS Office Tucson, Arizona, WR Technical*, 10–13.

Fagherazzi, S., & Wiberg, P. (2009). Importance of wind conditions, fetch, and water levels on wave-generated shear stresses in shallow intertidal basins. *Journal of Geophysical Research: Earth Surface*, *114*(F3).

García-Díez, M., Fernández, J., Fita, L., & Yagüe, C. (2013). Seasonal dependence of wrf model biases and sensitivity to pbl schemes over europe. *Quarterly Journal of the Royal Meteorological Society*, *139*(671), 501–514.

Hegarty, J. D., Lewis, J., McGrath-Spangler, E. L., Henderson, J., Scarino, A. J., DeCola, P., ... Welton, E. J. (2018). Analysis of the planetary boundary layer height during discover-aq baltimore–washington, dc, with lidar and high-resolution wrf modeling. *Journal of Applied Meteorology and Climatology*, *57*(11), 2679–2696.

Homer, C. H., Fry, J. A., & Barnes, C. A. (2012). The national land cover database. *US Geological Survey Fact Sheet*, *3020*(4), 1–4.

Ishigami, A., Hajat, S., Kovats, R. S., Bisanti, L., Rognoni, M., Russo, A., & Paldy, A. (2008). An ecological time-series study of heat-related mortality in three european cities. *Environmental Health*, *7*(1), 1–7.

Lee, D. O. (1984). Urban climates. *Progress in Physical Geography*, *8*(1), 1–31.

Li, D., Malyshev, S., & Shevliakova, E. (2016). Exploring historical and future urban climate in the earth system modeling framework: 2. impact of urban land use over the continental united states. *Journal of Advances in Modeling Earth Systems*, *8*(2), 936–953.

McPhearson, T., Iwaniec, D. M., & Bai, X. (2016). Positive visions for guiding urban transformations toward sustainable futures. *Current opinion in environmental sustainability*, *22*, 33–40.

Menne, M. J., Durre, I., Korzeniewski, B., McNeal, S., Thomas, K., Yin, X., ... Houston, T. G. (2012). Global historical climatology network - daily (GHCN-Daily), version 3.
doi: doi:10.7289/V5D21VHZ

Mesinger, F., DiMego, G., Kalnay, E., Mitchell, K., Shafran, P. C., Ebisuzaki, W., ... others (2006). North american regional reanalysis. *Bulletin of the American Meteorological Society*, *87*(3), 343–360.

Mikolaskova, K. (2009). Continental and oceanic precipitation régime in europe. *Central European Journal of Geosciences*, *1*(2), 176–182.

Murray, F. W. (1966). *On the computation of saturation vapor pressure* (Tech. Rep.). Rand Corp Santa Monica Calif.

Oke, T. R. (1988). Street design and urban canopy layer climate. *Energy and buildings*, *11*(1-3), 103–113.

Oleson, K. W., Bonan, G. B., Feddema, J., Vertenstein, M., & Kluzek, E. (2010). Technical description of an urban parameterization for the community land model (CLMU). *NCAR, Boulder*.

Oliveira, V. (2016). *Urban morphology: an introduction to the study of the physical form of cities*. Springer.

OpenDataDC. (2021). *Open Data DC.* D.C. Office of the Chief Technology Officer (OCTO). Retrieved from `https://opendata.dc.gov/datasets`

Pan, L., Liu, Y., Knievel, J., Delle Monache, L., & Roux, G. (2018). Evaluations of WRF sensitivities in surface simulations with an ensemble prediction system. *Atmosphere*, *9*(3), 106.

Reza, H. M. (2019). Study on changes in micro-climatic parameters and domestic energy consumption influenced by changes in urban morphology in hatirjheel area, dhaka.

Samenow, J. (2012). The longest, strongest heat wave: D.C. records 9th straight 95+ day. *The Washington Post*. Retrieved from `https://www.washingtonpost.com/blogs/capital-weather-gang/post/the-longest-strongest-heat-wave-dc-records-9th-straight-95-day/2012/07/06/gJQA1hU1RW_blog.html`

Sapena, M., & Ruiz, L. A. (2015). Analysis of urban development by means of multi-temporal fragmentation metrics from LULC data. *The International Archives of Photogrammetry, Remote Sensing and Spatial Information Sciences*, *40*(7), 1411.

Scheitlin, K. (2013). The maritime influence on diurnal temperature range in the chesapeake bay area. *Earth Interactions*, *17*(21), 1–14.

Shahmohamadi, P., Che-Ani, A., Maulud, K., Tawil, N., & Abdullah, N. (2011). The impact of anthropogenic heat on formation of urban heat island and energy consumption balance. *Urban Studies Research*, *2011*.

Vahmani, P., Jones, A. D., & Patricola, C. M. (2019). Interacting implications of climate change, population dynamics, and urban heat mitigation for future exposure to heat extremes. *Environmental Research Letters*, *14*(8), 084051.

Wang, Z.-H., Bou-Zeid, E., Au, S. K., & Smith, J. A. (2011). Analyzing the sensitivity of WRF's single-layer urban canopy model to parameter uncertainty using advanced monte carlo simulation. *Journal of Applied Meteorology and Climatology*, *50*(9), 1795–1814.

Weather Underground. (2010). *Weather observations, 2010.* `https://www.wunderground.com/history/daily/us/va/arlington-county/KDCA/date/2010-7-6`.

Wedi, N. P. (2014). Increasing horizontal resolution in numerical weather prediction and climate simulations: illusion or panacea? *Philosophical Transactions of the Royal Society A: Mathematical, Physical and Engineering Sciences*, *372*(2018), 20130289.

Werner, W., Kelly Wang. (2017). *Nesting in WRF.* `https://www.climatescience.org.au/sites/default/files/werner_nesting.pdf`.